

Reversible Deep Neural Network Watermarking: Matching the Floating-point Weights

Junren Qin, Fan Yang, Jiarui Deng and Shanxiang Lyu *

College of Cyber Security, Jinan University, Guangzhou 510632, China.

Abstract. Static deep neural network (DNN) watermarking embeds watermarks into the weights of DNN model by irreversible methods, but this will cause permanent damage to watermarked model and can not meet the requirements of integrity authentication. For these reasons, reversible data hiding (RDH) seems more attractive for the copyright protection of DNNs. This paper proposes a novel RDH-based static DNN watermarking method by improving the non-reversible quantization index modulation (QIM). Targeting the floating-point weights of DNNs, the idea of our RDH method is to add a scaled quantization error back to the cover object. Two schemes are designed to realize the integrity protection and legitimate authentication of DNNs. Simulation results on training loss and classification accuracy justify the superior feasibility, effectiveness and adaptability of the proposed method over histogram shifting (HS).

Keywords: deep neural network (DNN) · watermarking · reversible data hiding (RDH).

1 Introduction

Due to their remarkable performance, deep neural networks (DNNs) have been widely applied in many fields, such as image steganography [19], signal denoising [12], and so on. Watermarking DNNs is an important step in protecting the intellectual property embedded in these models [1]. With the increasing use of deep learning based systems, there is a risk that someone can use or modify the model without providing attribution to the original author. Watermarking adds an extra layer of security that allows the original author to prove ownership of the model and protect it from unauthorized access and use. Additionally, watermarking can be used to track the provenance of a model, ensure the integrity of the weights and parameters, facilitate model versioning and enable the identification of malicious models.

DNN watermarking is classified into static and dynamic watermarking depending on where the watermark can be read from [11]. i) For static watermarking (see, e.g., [7, 10, 16, 22]), the watermark can be read directly from the network

* The authors are with the College of Cyber Security, Jinan University, Guangzhou 510632, China . *Corresponding author: Shanxiang Lyu (lsx07@jnu.edu.cn).*

weights. The weights are determined during the training phase, and they are of floating-point formats, which differs from the popular unsigned-integer format of images. ii) For dynamic watermarking (see, e.g., [3, 9]), when fed with some crafted inputs, a dynamic watermark can alter the behavior of the network, which makes the watermark message visible in the model output.

An interesting research direction is to further endow a reversible property to DNN watermarks. Reversible watermarking is a type of digital watermarking that enables content owners to protect their digital data without causing any permanent modifications [5, 18]. This type of watermarking allows the embedded information to be retrieved from the host object without any data loss or damage. Focusing on the unsigned integer format of images, many celebrated reversible watermarking algorithms have been developed, such as difference expansion (DE) [21], prediction-error expansion (PEE) [20, 23], histogram shifting (HS) [15]. As the weights can be considered conventional multimedia objects, reversible watermarking of DNN is akin to a further development of static DNN watermarking, which embeds reversible watermarks over the weights. Recently Guan *et. al.* [4] employed HS to watermark the weights of convolutional neural networks (CNNs), where the weights are represented as the multiplicative factor of the filters. Yet HS is not a good fit for the floating-point weights. Actually [4] has to transform weights into integers for the sake of deploying HS. Moreover, HS deteriorates if the host admits a uniform or uniform-like distribution.

Against this background, it becomes tempting to design a reversible watermarking scheme that matches the floating-point weights in DNNs. The contributions of this paper, along with the highlights, are summarized as follows.

- First, without making assumptions on the distribution of the cover object, we design a simple yet efficient reversible watermarking algorithm by improving the celebrated quantization index modulation (QIM) [2], namely reversible QIM (R-QIM). For floating-point or real-valued objects, QIM resembles a lattice quantizer that maps input values from a large set (often a continuous set) to output values in a countable smaller set with a finite number of elements [13, 24]. The quantization in QIM is naturally lossy; however, as the cover-object is available while performing QIM, we can add a scaled version of the difference vector backed to the quantized output values, which makes the cover object reversible.
- Second, we explain how to deploy R-QIM in DNN watermarking, and realize integrity protection and legitimacy authentication via R-QIM based scheme. For integrity protection, the owner or trusted third-party institution can verify the occurrence of data tampering regardless of noiseless channel or known noisy channel, which solves the unavailability existing scheme had in noisy channel transmitting. For legitimacy authentication, the proposed scheme provides an effective way to distinguish the legal and illegal using of target DNNs. This provides a valuable layer of protection as it can help deter attackers, as well as identifying the individuals responsible for the attack. It also provides a means of verifying that a given DNN is authentic,

guaranteeing that the data it produces has not been compromised in any way.

- Third, theoretical justifications and numerical simulations are both presented to demonstrate the advantages of R-QIM. We analyze the signal to watermark ratio (SWR) of R-QIM which serves capacity and fidelity, and the impact of covers’ distributions in HS [4]. By analyzing the weights of multi-layer perceptron (MLP) and visual geometry group (VGG) models, we compare the training loss and classification accuracy of R-QIM and HS [4].

The rest of the paper is organized as follows. In Section 2, DNN watermarking models and existing algorithms are introduced. In Section 3 and Section 4, we present R-QIM along with theoretical analyses, as well as the applications of R-QIM. Simulation results and conclusions are given respectively in Section 5 and Section 6.

2 Preliminaries

2.1 Reversible DNN Watermarking Basics

Like static DNN watermarking [11, 22], reversible DNN watermarking also embeds the watermark into the weights of the DNN model. Such weights are determined during the training phase and assume fixed values that do not depend on the input of the network.

The mathematical model can be described as follows. Let \mathbf{W} be the whole weights in a general trained DNN model. For the watermark embedding, appropriate weights in \mathbf{W} are selected by a location sequence \mathbf{c} guided by a clue/key cl , which builds a cover sequence \mathbf{s} . To embed the information sequence \mathbf{m} into \mathbf{s} , as well as ensuring the subsequent correct extraction, one should judiciously design the following triplet:

$$\begin{cases} \mathbf{s}_w = \text{Emb}(\mathbf{s}, \mathbf{m}) \\ \hat{\mathbf{m}} = \text{Ext}(\mathbf{s}_w + \mathbf{n}) = \text{Ext}(\mathbf{y}) \\ \hat{\mathbf{s}} = \text{Rec}(\mathbf{s}_w + \mathbf{n}) = \text{Rec}(\mathbf{y}) \end{cases} \quad (1)$$

where $\text{Emb}(\cdot)$, $\text{Ext}(\cdot)$ and $\text{Rec}(\cdot)$ represent the embedding, extraction and recovering functions, respectively, while \mathbf{y} denotes the possibly noisy reception of the watermarked sequence \mathbf{s}_w (E.g., $\mathbf{y} = \mathbf{s}_w + \mathbf{n}$ for the case of additive noises).

While reversible DNN watermarking is similar to reversible image watermarking, they are different in terms of the cover formats, robustness and fidelity requirements. The comparison is summarized in Table 1.

2.2 Existing Methods

HS. HS is a reversible watermarking algorithm for images, and has been recently adjusted to deploy in CNNs[4]. The whole method is divided into three parts:

Table 1: The comparison of reversible image watermarking and reversible DNN watermarking

Features	Reversible image watermarking	Reversible DNN watermarking
Format of covers	Unsigned integers	Floating-point numbers
Fidelity	Higher quality of the host signal after watermark embedding	Higher effectiveness of the host network after watermark embedding
Capacity	The ability to embed watermark with a massive data/information	
Security	The ability to remain secret for unauthorized parties on watermark accessing, reading and modifying	
Efficiency	Higher speed for the embedding and extracting process of watermarking algorithm	

host sequence construction, data preprocessing and watermarking algorithm. The host sequence construction implies the method to construct a host matrix from a convolutional layer in CNN, which is irrelevant to this paper. In the data preprocessing, each weight is defined as

$$\omega = \pm 0.\underbrace{00\dots 0}_p n_1 n_2 \dots n_c n_{c+1} \dots n_q, \quad (2)$$

in which q represents the whole length of digits for the weight. To meet the requirements of integer host, the consecutive non-zero digit pairs (n_c, n_{c+1}) in ω , corresponding to the minimum entropy, is chosen as the significant digit pairs to construct the host sequence. Then, the chosen pairs will add an adjustable integer parameter V to adjust it for the appropriate range $[-99, 99]$.

For the watermarking algorithm, [4] chose HS [15] scheme as the embedding and extracting strategy. By defining the histogram peak of the whole ω as Ω_{\max} and the histogram valley Ω_{\min} , the 1-bit HS embedding for the watermark m can be described as

$$\omega' = \begin{cases} \omega + m, & \omega = \Omega_{\max} \\ \omega + 1, & \omega \in (\Omega_{\max}, \Omega_{\min}) \\ \omega, & \omega \notin [\Omega_{\max}, \Omega_{\min}) \end{cases}. \quad (3)$$

The histogram shift operation in this 1-bit embedding process is depicted in Fig. 1(a), where the bins more than Ω_{\max} are shifted towards right by fixed $\Delta = 1$ to create a vacant bin for embedding, and the watermark m of uniform distribution is embedded into the bin equal to Ω_{\max} by HS. This divides the whole cover into three regions depicted in Fig. 1 (c), in which the covers smaller than Ω_{\max} are referred to region i, the covers equal to Ω_{\max} to region ii, and the covers larger than Ω_{\max} to region iii. For each bit, ω changes by the mapping rule depicted in Fig. 1 (b).

With the same process of host sequence construction and data preprocessing, the extracting process can be described as

$$\hat{m} = \begin{cases} 1, & \omega' = \Omega_{\max} + 1 \\ 0, & \omega' = \Omega_{\max} \end{cases}, \quad (4)$$

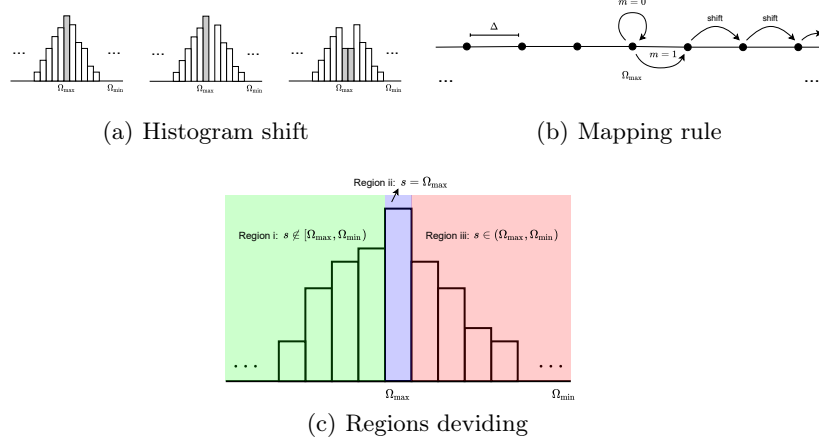


Fig. 1: Illustration of the HS algorithm [4].

and the recovering process

$$\hat{\omega} = \begin{cases} \omega' - 1, & \omega \in (\Omega_{\max}, \Omega_{\min}) \\ \omega', & \omega \notin [\Omega_{\max}, \Omega_{\min}) \end{cases}. \quad (5)$$

QIM. QIM is a popular method for non-reversible watermarking [14]. Its rationale can be explained by the example in Fig. 2(a). The circle and cross positions of Fig. 2(a) denote two sets A_0 and A_1 , and they are arranged alternately. Given a host/cover sample $s \in \mathbb{R}$ and a one-bit message $m \in \{0, 1\}$, the watermarked value is simply moving s to the nearest point in A_0 when $m = 0$, and to the nearest point in A_1 when $m = 1$.

Define $Q_{\Delta}(s) = \Delta \lfloor s/\Delta \rfloor$ with Δ being a step-size parameter. Then the embedding process can be described as

$$s_{\text{QIM}} \triangleq Q_m(s) = Q_{\Delta}(s - d_m) + d_m, \quad m \in \{0, 1\}, \quad (6)$$

where $d_0 = -(\Delta/4)$, $d_1 = \Delta/4$, $A_0 = d_0 + \Delta\mathbb{Z}$ and $A_1 = d_1 + \Delta\mathbb{Z}$.

Assume that the transmitted s_{QIM} has undergone the contamination of an additive noise term n , then at the receiver's side we have: $y = s_{\text{QIM}} + n$. A minimum distance decoder is therefore given as

$$\hat{m} = \arg \min_{m \in \{0, 1\}} \left[\min_{s \in A_m} |y - s| \right]. \quad (7)$$

If $|n| < \Delta/4$, the \hat{m} is correct.

Regarding the embedding distortion, as shown in Fig. 3(a), the maximum error caused by embedding is $\Delta/2$. If the quantization errors are distributed

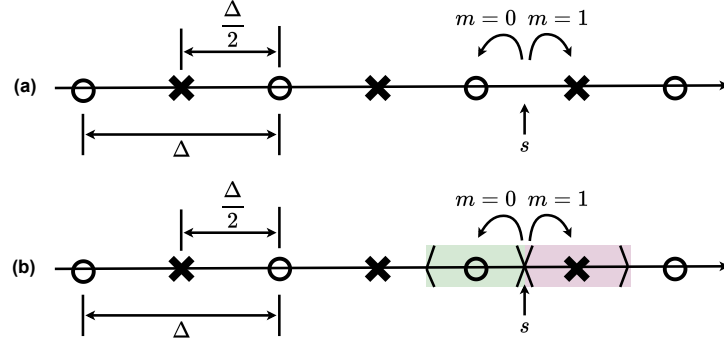


Fig. 2: Embed one bit into a sample with different versions of QIM. (a) Conventional QIM. (b) Reversible QIM.

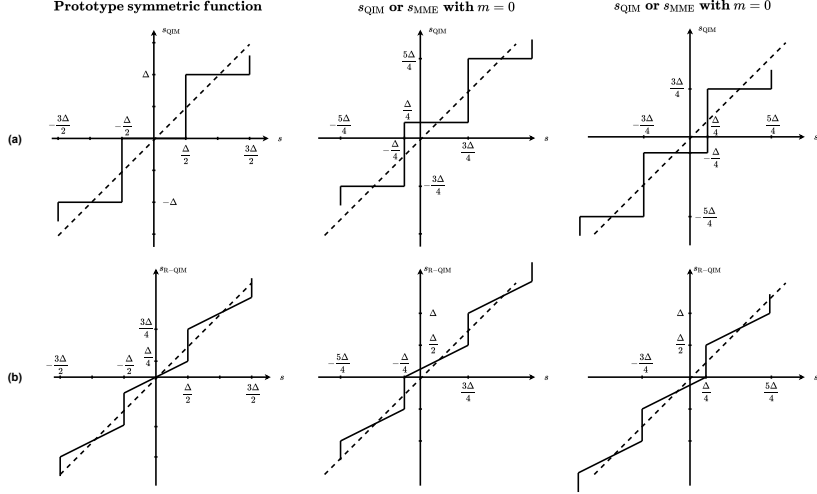


Fig. 3: Selection of watermarked signal with given s and $m \in \{0, 1\}$ for Prototype symmetric function, $x = Q_m(s)$ with $m = 0$, and $x = Q_m(s)$ with $m = 1$ in different one-bit watermarking. (a) Conventional QIM. (b) Reversible QIM with $\alpha = 0.5$.

uniformly over $[-(\Delta/2), (\Delta/2)]$, then the mean-squared embedding distortion is $D = \Delta^2/12$. Considering the capacity, QIM is almost 1 bpps which means each sample of host cover can remain 1 sample of watermark.

3 THE PROPOSED METHOD

Notice that floating-point arithmetic is arithmetic that represents real numbers approximately. As QIM can work with the Euclidean domain, this section presents a QIM-based RDH algorithm named reversible QIM (R-QIM), and elaborate its advantages compared to [4].

3.1 R-QIM

We observe that there exists a quantization error e between the cover vector s and its quantized watermarked vector $Q_{(m,k)}(s)$, i.e.,

$$e = s - Q_m(s). \quad (8)$$

Obviously the information about e is lost if we only use $Q_m(s)$ as the watermarked vector. Notice that QIM has certain error tolerance capability. If we treat e as the “beneficial noise” and add it back to $Q_m(s)$, then the information about the cover s can be maintained, and the scheme becomes reversible. The tricky part about adding “beneficial noise” is that, they should be properly scaled to meet several demands. First, the scaled e should be small enough such that it does not go beyond the correct decoding region. Second, the scaled e should not be too small to avoid exceeding the used representation accuracy of numbers.

The method incorporating the above ideas is referred to as R-QIM. Its embedding operation is defined as

$$s_{\text{R-QIM}} \triangleq \alpha Q_{(m,k)}(s) + (1 - \alpha)s, \quad (9)$$

where α denotes a scaling factor satisfying $\alpha \in \left(\frac{|\mathcal{M}|-1}{|\mathcal{M}|}, 1\right)$, $Q_{(m,k)}(s)$ represents a encrypted quantizer defined as

$$Q_{(m,k)}(s) \triangleq Q_{\Delta}(s - d_m - k) + d_m + k, m \in \mathcal{M}. \quad (10)$$

In Eq. (10), $Q_{\Delta}(s)$ denotes the same $Q_{\Delta}(s) = \Delta \lfloor s/\Delta \rfloor$ as conventional QIM, and k a dithering component for secrecy. With reference to Eqs. (9) (10), R-QIM can be regarded as a fast version of our lattice-based method in [17].

Since k and α respectively relate to the correctness of decoding and recovering, they usually act as secret keys in a watermarking scheme. By setting $k = 0$ and $\alpha = 0.5$, the 1-bit embedding example of R-QIM is depicted in Fig. 2(b), in which watermarked covers are distributed in the green and red zone around the circle and cross positions, rather than the positions of their points.

For receiver, the estimated watermark can be extracted from his received y by

$$\hat{d}_m \equiv Q_{\frac{\Delta}{|\mathcal{M}|}+k}(y) = \left[Q_{\frac{\Delta}{|\mathcal{M}|}}(y - k) + k \right] \{\Delta\}. \quad (11)$$

When the noise term n is small enough to satisfy

$$Q_{\frac{\Delta}{|\mathcal{M}|}+k}(n) = 0, \quad (12)$$

correct extraction $\hat{d}_m = d_m$ occurs, regardless in noiseless or noisy channel.

To estimate the original weight s from the received y , we have

$$\hat{s} = \frac{y - \alpha Q_{\frac{\Delta}{|\mathcal{M}|} + k}(y)}{1 - \alpha}. \quad (13)$$

Notice that the correct restoration $\hat{s} = s$ occurs if and only if $n = 0$, *s.t.*, $y = s_{\text{R-QIM}}$. If the channel is noisy, the error of estimation is

$$\hat{s} - s = \frac{n}{1 - \alpha}. \quad (14)$$

By setting $\alpha = 0.5$ and $k = 0$, the embedding distortion is depicted in Fig. 3(b), whose maximum error is $\alpha\Delta/2 = \Delta/4$. If the quantization errors are distributed uniformly over $[-(\Delta/2), (\Delta/2)]$, then the mean-squared embedding distortion is

$$D = \frac{\alpha}{12} \Delta^2. \quad (15)$$

Obviously, since $\bigcup_{m=0}^{|\mathcal{M}|-1} \Lambda_m = \mathbb{R}$ (as shown in Fig. 2), each bit of watermark can embed into a sample of host with any characteristic and distribution. Such features make R-QIM possessing almost the same maximum length of available watermark as the number of host samples.

3.2 Discussions

Compared to HS [4], R-QIM is more suitable for RDH-based static DNN watermarking in terms of usability, capacity and imperceptibility. To confirm this conclusion, respectively in this subsection, we analyze the HS-based scheme in [4] and the theoretical advantages of R-QIM seriously. We consider that all the host sequence constructed from the whole weights of DNN model is a piece of real number bit flow of normal distribution.

In terms of usability, HS mismatches the host of uniform distribution for two reasons:

- i) There are some obvious statistical characteristics of the watermarked sequence produced from the uniform host, which is defenseless against the passive attack.
- ii) The low capacity of HS becomes worse and unbearable in uniformly distributed host.

Therefore, HS seems not feasible as the data preprocessing operation makes the host sequence uniform rather than being normal distributed. For the data preprocessing operation, different random 10000 length data of normal distribution are tested 1000 times on skewness, kurtosis and Kolmogorov–Smirnov (K-S) test, and one of them is tested by Quantile-Quantile (Q-Q) plot. The results are depicted in Fig. 4 where the preprocessed data become flatter, and disobey normal distribution in K-S test. In Fig. 4(d), (e) and (f), the observations imply that the preprocessed data is consistent distribution with the uniform random integer

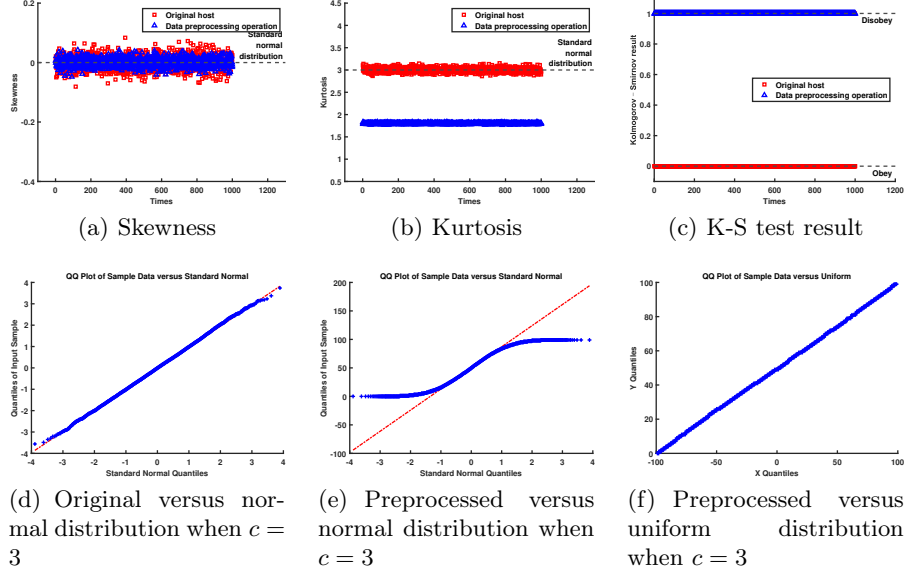


Fig. 4: Skewness, Kurtosis and K-S test results on normal distribute data, and their respective Q-Q plots.

flow of the same range. Thus, HS [4] lacks practical usability, while the R-QIM is feasible for data admitting any distribution.

Regarding the theoretical advantages of R-QIM, we analyze the capacity and imperceptibility for R-QIM and the HS. To evaluate the embedding capacity, we consider a host sequence of length L to analyze the maximum available watermark length C_{\max} by implementing R-QIM and HS. To evaluate the imperceptibility, since the effectiveness of the host network is difficult to measure in theory, we assume it is proportional to lower embedding distortion, and this assumption is verified in the experiments. To evaluate the embedding distortion, the popular signal to watermark ratio (SWR) is defined as

$$\text{SWR (dB)} = 10 \times \lg \left(\frac{\sigma_s^2}{\sigma_w^2} \right), \quad (16)$$

where σ_s^2 , σ_w^2 represent the power of the host and the additive watermark, respectively. Because of the same host, a smaller σ_w^2 leads to a higher SWR implied better performance on imperceptibility. For the fairness of the distortion analysis, we assume the same capacity and host distribution for both HS in [4] and R-QIM, corresponding to embed watermark into the host equal to Ω_{\max} which follows Gaussian distribution and depicts in Fig. 1 (c).

Considering the embedding capacity, since the watermark only embeds into the bin of $s = \Omega_{\max}$ via the HS method in [4], and the other bins contain no information of watermarks, the maximum length of available watermark in HS

can be calculated by

$$C_{\max, \text{HS}} = \Pr(X \in \text{Region } ii) \cdot L. \quad (17)$$

However, in R-QIM, the whole host sequence can embed the watermark, which implies that $C_{\max, \text{R-QIM}} = L$. Obviously, for the same length of host sequence, R-QIM has higher embedding capacity.

In terms of the embedding distortion, we have the following result.

Theorem 1. *R-QIM has a larger SWR than HS when $\Delta \leq \sqrt{3}$.*

Proof. Due to the symmetry of Gaussian distribution that $\Pr(X \in \text{Region } i) = \Pr(X \in \text{Region } iii)$, we have $\Pr(X \in \text{Region } ii) = 1 - 2\Pr(X \in \text{Region } iii)$. With the same setting, the $\sigma_{\mathbf{w}}^2$ of HS is

$$\begin{aligned} \sigma_{\mathbf{w}, \text{HS}}^2 &= \frac{1}{4} \Pr(X \in \text{Region } ii) + \Pr(X \in \text{Region } iii) \\ &= \frac{1}{4} + \frac{1}{2} \Pr(X \in \text{Region } iii), \end{aligned} \quad (18)$$

while $\sigma_{\mathbf{w}}^2$ of R-QIM is

$$\begin{aligned} \sigma_{\mathbf{w}, \text{R-QIM}}^2 &= \frac{\alpha \Delta^2}{12} \Pr(X \in \text{Region } ii) \\ &= \frac{\alpha \Delta^2}{12} - \frac{\alpha \Delta^2}{6} \Pr(X \in \text{Region } iii). \end{aligned} \quad (19)$$

Based on Eqs. (18) and (19), we have

$$\sigma_{\mathbf{w}, \text{HS}}^2 - \sigma_{\mathbf{w}, \text{R-QIM}}^2 = \frac{3 - \alpha \Delta^2}{12} + \frac{3 + \alpha \Delta^2}{6} \Pr(X \in \text{Region } iii). \quad (20)$$

Since $0 < \Pr(\text{Region } iii) < 1/2$, one has

$$\frac{3 - \alpha \Delta^2}{12} < \frac{3 - \alpha \Delta^2}{12} + \frac{3 + \alpha \Delta^2}{6} \Pr(X \in \text{Region } iii) < \frac{1}{2}. \quad (21)$$

Eq. (20) is larger than 0 when $\Delta \leq \sqrt{3}$, so the theorem is proved.

According to Theorem 1, for the same fixed setting of $\Delta = 1$ in HS [4], we can observe that R-QIM obtains a lower embedding distortion, and better fidelity based on aforementioned assumption. On the other hand, it also indicates that the fidelity of R-QIM can be controlled. When $\Delta > \sqrt{3}$, by setting parameters artificially, we can obtain flexible performance of fidelity, regardless better or worse than HS. In the scheme designing we will demonstrate the benefits of this.

Algorithm 1 Mark

Input: Trained Model \mathbf{W} , Watermark \mathbf{m} , Scaling Factor α , Dithering Vector k , Embedding Clue cl , Step Size Δ

Output: Watermarked Model \mathbf{W}_{wtm} , Watermark Information $\mathbf{w_info}$, Secret Key \mathbf{sk}

```

1:  $[L, |\mathcal{M}|] \leftarrow \text{Info}(\mathbf{m})$ 
2:  $\mathbf{c} \leftarrow \text{Construction}(cl, L)$ 
3:  $\mathbf{W}_{wtm} \leftarrow \mathbf{W}, i \leftarrow 0$ 
4: for  $++i \leq L$  do
5:    $s_i \leftarrow \mathbf{W}(\mathbf{c}(i))$ 
6:    $m_i \leftarrow \mathbf{m}(i)$ 
7:    $\mathbf{W}_{wtm}(\mathbf{c}(i)) \leftarrow \text{Emb}(s_i, m_i, \alpha, k, \Delta)$ 
8:  $\mathbf{w\_info} \leftarrow [L, |\mathcal{M}|]$ 
9:  $\mathbf{sk} \leftarrow [k, cl, \Delta]$ 

```

4 Applications of R-QIM

In this section, we deploy R-QIM in static DNN watermarking. The proposed scheme contains several algorithms realizing the embedding, extracting and recovering process. Then, the concrete steps of some functions, including integrity protection and infringement identification, are elaborated for realizing via proposed scheme. The schematics of the two applications are depicted in Fig 5. The owner of DNNs, legal user, illegal user and trusted third-party institution are respectively named as "Alice", "Bob", "Mallory" and "Institution" for the sake of simplicity.

4.1 Wrapping-up R-QIM

R-QIM should be additional wrapped-up for security concerns. Based on R-QIM, the processes of watermarking, extracting and restoring are displayed by pseudo-codes of **Mark**, Algorithm 1, **Extract**, Algorithm 2 and **Restore**, Algorithm 3. In these algorithms, some parameters included cl and k are set by a pseudo random number generator (PRNG), and the others, like step size Δ and scaling factor α , are set by the owner.

In **Mark** (Algorithm 1), trained model \mathbf{W} , watermark \mathbf{m} and the aforementioned parameters are regarded as the inputs to output the watermarked model \mathbf{W}_{wtm} and some side information which includes watermark information $\mathbf{w_info}$ and secret key \mathbf{sk} . After selecting a sequence $\mathbf{s} = [s_0, s_1, \dots, s_{L-1}]$ with the clue cl and obtaining some information (L and $|\mathcal{M}|$) from \mathbf{m} by Info function, each bit of watermark m_i will be embedded into s_i by employing Eq. (9) as $\text{Emb}(\cdot)$. Then, L and $|\mathcal{M}|$ will be combined as $\mathbf{w_info}$, and cl , k and Δ as \mathbf{sk} . To ensure the security properties of the embedded watermark, DNN model's owner should keep $\mathbf{w_info}$, \mathbf{sk} and α in order not to divulge them.

Extract (Algorithm 2) realizes watermark extraction from the watermarked model \mathbf{W}_{wtm} produced by **Mark**. With the aid of watermark information $\mathbf{w_info}$

Algorithm 2 Extract**Input:** Watermarked Model \mathbf{W}_{wtm} , Watermark Information $\mathbf{w_info}$, Secret Key \mathbf{sk} **Output:** Extracted Watermark $\hat{\mathbf{m}}$

```

1:  $[L, |\mathcal{M}|] \leftarrow \mathbf{w\_info}$ 
2:  $[\alpha, k, cl, \Delta] \leftarrow \mathbf{sk}$ 
3:  $\mathbf{c} \leftarrow \text{Construction}(cl, L)$ 
4:  $i \leftarrow 0$ 
5: for  $++i \leq L$  do
6:    $y_i \leftarrow \mathbf{W}_{wtm}(\mathbf{c}(i))$ 
7:    $d_i \leftarrow \text{Ext}(y_i, k, \Delta, |\mathcal{M}|)$ 
8:    $\hat{\mathbf{m}}(i) \leftarrow \text{Codebook}(d_i)$ 

```

Algorithm 3 Restore**Input:** Watermarked Model \mathbf{W}_{wtm} , Watermark Information $\mathbf{w_info}$, Secret Key \mathbf{sk} , Scaling Factor α **Output:** Recovered Model $\hat{\mathbf{W}}$

```

1:  $[L, |\mathcal{M}|] \leftarrow \mathbf{w\_info}$ 
2:  $[\alpha, k, cl, \Delta] \leftarrow \mathbf{sk}$ 
3:  $\mathbf{c} \leftarrow \text{Construction}(cl, L)$ 
4:  $\hat{\mathbf{W}} \leftarrow \mathbf{W}_{wtm}, i \leftarrow 0$ 
5: for  $++i \leq L$  do
6:    $y_i \leftarrow \mathbf{W}_{wtm}(\mathbf{c}(i))$ 
7:    $\hat{\mathbf{W}}(\mathbf{c}(i)) \leftarrow \text{Rec}(y_i, k, \alpha, \Delta, |\mathcal{M}|)$ 

```

and secret key \mathbf{sk} kept by the owner, an estimated $\hat{\mathbf{d}}$ is created by employing Eq. (11) as $\text{Ext}(\cdot)$ after the same selecting process as **Mark**. Then, guided by watermark information in code book, **Extract** outputs an estimated watermark $\hat{\mathbf{m}}$ from $\hat{\mathbf{d}}$. Significantly, since watermark extraction need the assistance of secret key \mathbf{sk} rather than α related to the security of DNN model recovering, **Extract** should be implemented by the DNN model owner or a trustworthy third-party institution while ensuring the nondisclosure of scaling factor α .

Restore (Algorithm 3) takes the watermarked model \mathbf{W}_{wtm} as input to recover it into its original type, in which the watermark information $\mathbf{w_info}$, secret key \mathbf{sk} and scaling factor α act as the side information to aid the recovering process. After the same selecting process as **Mark**, each sample y_i is recovered to s_i one by one by employing Eq. (13) as $\text{Rec}(\cdot)$. Since correct restoration is related to noise term n , we can judge the tampering of watermarked model under noiseless channel or known noisy channel, which makes reversible watermarking to protect the integrity of watermarked model. Meanwhile, since the watermark contained in watermarked DNN model no more exists in restored model after **Restore**, we can evaluate the enforcement of recovering process by verifying the existence of watermark in a DNN model.

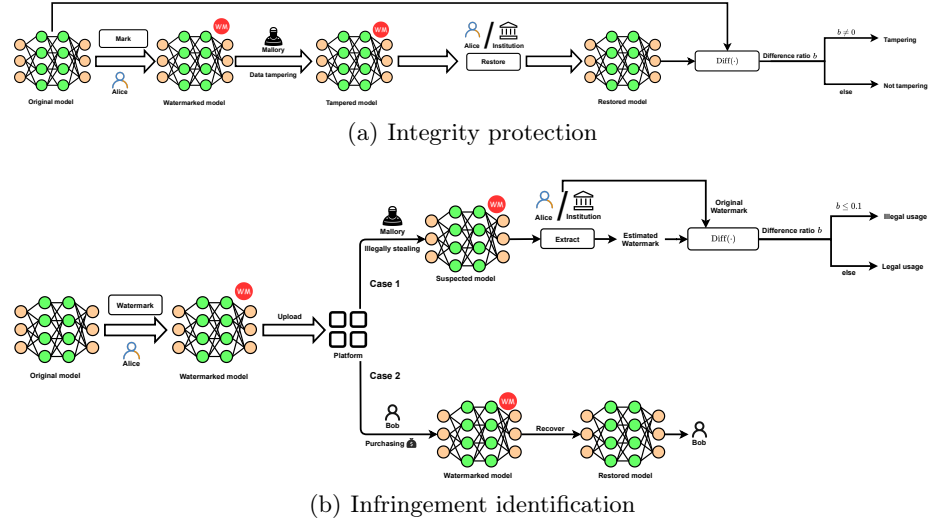


Fig. 5: Schematics of using R-QIM for integrity protection and infringement identification.

4.2 Integrity protection

For the reason of enabling a reversible property to DNN watermarks, [4] has introduced the integrity protection of DNN model, in which a scheme has been proposed to verify whether a DNN is tampered by comparing the bit difference of weights between the restored and the original models. In a similar vein to [4]’s, an integrity protection scheme employing R-QIM is depicted in Fig. 5 (a). In the figure, Alice embeds her watermarks into a commercialized DNN model \mathbf{W} via the **Mark** algorithm, and outputs a watermarked DNN model \mathbf{W}_{wtm} . During the process of transmission, Mallory illegally intercepts \mathbf{W}_{wtm} , tampers its weights, and shares it in profits. For the sake of identifying tampering, we define two types of operations for noiseless or noisy channels.

- **Noiseless channel.** Since correct recovering is guaranteed, the tampered DNN model is recovered by **Restore** to obtain an estimated model. Notably, since Eq. (13) contains $Q_{\frac{\Delta}{|\mathcal{M}|}+k}(y)$, which can be regarded as watermark extraction. Thus the **Restore** function can meet the demand of perfect recovery after watermark extraction. At last, the weights between the restored and the original models are compared via a difference function $\text{Diff}(\cdot)$, which outputs a difference ratio b . Due to the sensitiveness of the recovering process, minor changes of \mathbf{W}_{wtm} would lead to a difference on the weights of restored model. This feature makes it possible for integrity judgment, in which $b = 1$ (or $b = 0$) implies that \mathbf{W}_{wtm} has (not) been tampered.
- **Noisy channel.** Tampering of DNN models can be identified when the noise term n is small enough. Thanks to Eq. (14), we can measure the difference

between the restored and the original models in theory, such that the comparison in $\text{Diff}(\cdot)$ can proceed excluding the interference of noise term n . In this scenario, we compute the theoretical difference between the restored and the original models by Eq. (14), compare the theoretical difference, and obtain a difference ratio b . When $b = 1$ (or $b = 0$), it implies that \mathbf{W}_{wtm} has (not) been tampered.

Summarizing the above, our proposed scheme seems more suitable for the scenario of integrity protection when compared to [4]. In our scheme, the fidelity of \mathbf{W}_{wtm} is higher, which is justified by Theorem 1. In addition, our scheme is perhaps the first one to protect the integrity of \mathbf{W}_{wtm} over noisy channels.

4.3 Infringement identification

In addition to integrity protection, reversible DNN watermarking can achieve infringement identification for suspicious DNN models. Since recovering operation removes the watermark contained in watermarked DNN models, there exist no more watermark detected in the restored model. If a legal user holds the restored model while the illegal user holds the watermarked one, it becomes possible to distinguish them. Based on this idea, we propose a novel scheme for the infringement identification of DNN models, in which a user receives the secret key for recovering after legalization and obtains a restored model. The whole process of the proposed scheme of legitimate authentication are depicted in Fig. 5(b). For simplicity, the owner, legal user, illegal user and trusted third-party institution are respectively named as "Alice", "Bob", "Mallory" and "Institution".

In the proposed scheme, a commercialized DNN model \mathbf{W} , owned by Alice, is sold via a online/offline platform, and employs our proposed scheme to mark the ownership of \mathbf{W} . After Alice embeds a watermark into \mathbf{W} by **Mark**, the produced watermarked model \mathbf{W}_{wtm} is sent to the platform, and acts as an exhibit or trial product to promote Alice's model. Obviously, since the embedding process is deployed after model training, the fidelity of \mathbf{W}_{wtm} is worse so that its disclosure does not damage Alice's rights. Once the product has attracted Bob, both $\mathbf{w_info}$, \mathbf{sk} and α are sent from Alice to Bob, and Bob can recover \mathbf{W}_{wtm} into its original type via **Restore**. At that time, the recovered model is the same as original model so that it has the best effectiveness, and the watermark is removed totally so that the watermark is undetected in the recovered model. When Mallory illegally steals the DNN model on public platforms, Alice can initiate arbitration to an Institution after being learned. To authenticate the legitimacy of the suspicious model held by Mallory, Alice or the Institution can extract the estimated watermark $\hat{\mathbf{m}}$ from suspect model via **Extract**. Then, $\hat{\mathbf{m}}$ will be compared with Alice's watermark via $\text{Diff}(\cdot)$ which outputs a difference ratio b to detect the existence of embedded watermark. When $b \leq 0.1$, the watermark is regarded as detected, and Mallory is confirmed as illegal user.

To avoid damage Alice's rights, the DNN watermarking scheme for infringement identification should feature a small fidelity such that the effectiveness of watermarked model is no better than the original one. Thanks to Theorem 1,

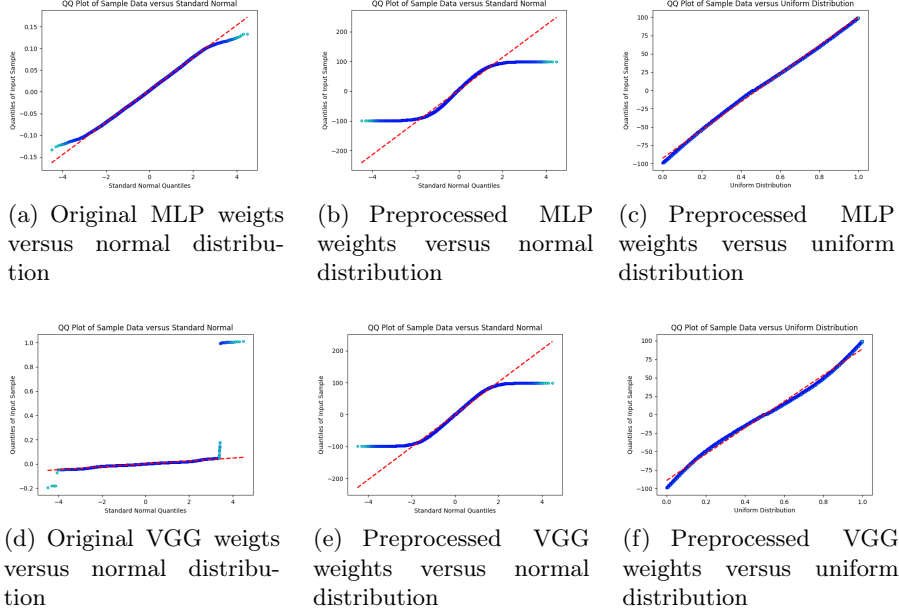


Fig. 6: Q-Q plot on the original and preprocessed weights with $c = 3$

R-QIM enjoys a bigger distortion than HS [4] by setting $\Delta > \sqrt{3}$ and a proper α , which can infer that R-QIM is more adaptable for the scenario of infringement identification.

5 SIMULATIONS

In order to evaluate the effectiveness of the proposed R-QIM scheme, simulations are divided into three parts: i) The usability of the HS method in [4]. ii) The comparison between R-QIM and HS on the capacity and fidelity. iii) The impact of parameters of R-QIM. The setups in these experiments are summarized as follows.

Datasets and Models: In the experiments, **MNIST** [8] and **CIFAR10** [6] are chosen as the datasets to train the Multi-layer Perceptron (MLP) model and the Visual Geometry Group (VGG) model respectively. **MNIST** is a handwritten digits data set in which 60,000 training and 10,000 testing gray-scale images with a size of 28×28 pixels are divided into 10 classes. With the same 10 classes of figures, **CIFAR10** contains 50,000 training and 10,000 testing color images of the size 32×32 pixels. In the experiments, the models and datasets are divided into two combinations, that is, the MLP model with **MNIST**, referred to as group A, and the VGG model with **CIFAR10**, referred to as group B.

Table 2: The analysis of weights in different models

Metric	MLP (198656 length)		VGG (200000 length)	
	Original	Preprocessed	Original	Preprocessed
Skewness	0.0426	-0.1059	34.8544	-0.0028
Kurtosis	2.8642	1.8324	1692.39	1.8276
$P \leq 5\%$ in K-S test	×	×	×	×
$P \leq 5\%$ in J-B test	×	×	×	×

Parameters: A piece of text converted to the bit stream is selected as the watermark. We set the step size $\Delta = 1$, and choose the same scaling factor $\alpha = 0.8675$ and dithering value $k = 0$.

Indicators: To evaluate the fidelity of the watermarked model, we apply training loss and classification accuracy as the metrics, in which the former measures the embedding damage, and the latter weighs the effectiveness of the watermarked network. A lower training loss indicates less impact from watermark embedding, while a higher classification accuracy reflects the greater effectiveness of the watermarked network. To detect the existence of copyright information and tampering detection, the bit error rate (BER) is employed as the metric which is defined as

$$BER = \frac{\sum_{k=1}^N (x_k \oplus x'_k)}{N}, \quad (22)$$

where x_k and x'_k separately denote the k -th bit of the original and estimated message. In copyright protection, information exists if BER is not larger than 10%, otherwise not. For the detection of tampering, a model is said to be untampered if BER equals to 0.

5.1 Usability test

We have theoretically identified potential weakness of HS in section 3.2. To support our claims, we conduct a numerical analysis of the weights of DNN models.

Fig. 6 shows the Q-Q plot on the original and preprocessed weights of MLP and VGG models versus normal and uniform distribution. The original weights of two models have a closer shape to the normal distribution, and the preprocessed weights of two models are obviously both the integer of uniform distribution rather than normal distribution.

Additionally, we analyzed the skewness, kurtosis, K-S test, and Jarque-Bera (J-B) test results for the original and preprocessed weights of MLP and VGG, and summarized them in Table 2, indicating that: i) The data preprocessing flattens the data distribution, resulting in lower kurtosis values for the preprocessed weights. ii) Neither the original nor the preprocessed weights of MLP and VGG pass the K-S and J-B tests. Above experiments demonstrate that realistic DNN weights do not follow a normal distribution, but this does not affect the validity of the data preprocessing method proposed in [4] for transforming data from

Table 3: Maximum capacity versus the HS method in [4]

Host length	MLP (198656 length)		VGG (200000 length)	
	R-QIM	HS[4]	R-QIM	HS[4]
20%	39732	377	40000	396
40%	79463	811	80000	760
60%	119194	1187	120000	1177
80%	158925	1565	160000	1604
100%	198656	1969	200000	1982

normal to uniform distribution. Nonetheless, this highlights the limited usability of the [4] method.

5.2 Capacity and fidelity comparisons

Regarding the adaptability of two proposed schemes for capacity and fidelity, we design several experiments to verify the superiority of R-QIM in two applications. The first application, integrity protection, requires a watermarking method with high embedding capacity and little embedding damage. Thus, we compare the maximum available capacity, classification accuracy, and training loss between our proposed scheme and [4]’s with the fixed $\Delta = 1$.

Considering the maximum available capacity, table 3 shows a considerable difference between R-QIM and HS. Regardless of group A or B, the table implies that R-QIM has a higher embedding capability than the benchmark method, which is consistent with our theoretical analysis.

As for fidelity, we compare the training loss and classification accuracy of the watermarked model embedded in different epochs by R-QIM and HS. Some results are presented in Fig. 7(a)-(d), where R-QIM outperforms the benchmark method in both metrics for group A and B, and group B is more obvious than A. Notably, observations in Fig. 7(a)-(d) also support our assumption that lower embedding distortion leads to better fidelity of watermarked model.

Regarding infringement identification, according to theorem 1, R-QIM can obtain a more obvious decline in fidelity than HS by setting $\Delta > \sqrt{3}$. To verify this, the classification accuracy and training loss of MLP and VGG model with different α and Δ are respectively depicted in Fig. 7(e)-(h), in which we draw the following observations: i) As α and Δ increase, the loss of watermarked model increases while the accuracy decreases, which aligns with our expectation under the assumption between distortion and fidelity. ii) When $\Delta = 1 < \sqrt{3}$ in R-QIM, it outperforms HS in terms of both loss and accuracy for groups A and B. However, when $\Delta = 3, 5 > \sqrt{3}$, HS is better than R-QIM. This supports theorem 1, and demonstrates the flexibility of performance of R-QIM which determines the applicability in infringement identification.

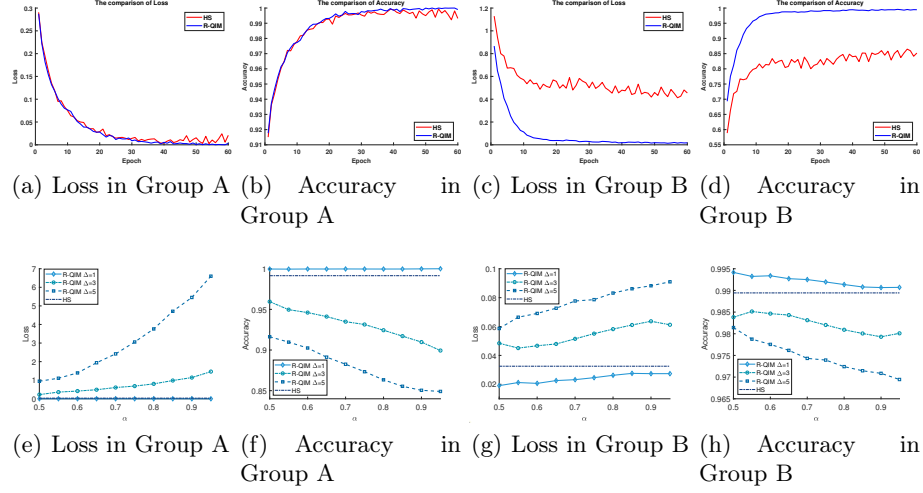


Fig. 7: Loss and Accuracy versus HS [4] with different (a)-(d) epochs. (e)-(h) α and Δ .

5.3 Performance of R-QIM recovering

We construct several simulations to explore the performance of R-QIM recovering, including the accuracy of recovered value and the presence of watermarks. Notably, the watermarks in these experiments are converted to uniform data consisting of 4264 bits.

In the first experiment, we aim to compare the performance difference in implementing reversible operations. We train two combinations from scratch twice for 60 epochs and embed watermark at epoch 30 via the proposed scheme. In first time (denoted by green line), reversible operation is applied immediately after the embedding process, but not in second time (denoted by red line). From Fig. 8(a), (b), we can obtain some notable observations. i) After watermark embedding, the model's accuracy sharply degrades due to the parameter modification. However, with the implementation of the proposed reversible operation, the reduced accuracy immediately restores. This shows the effectiveness of the reversible operation in offsetting the damages caused by the watermark embedding. ii) When reduced accuracy steps into a plateau without reversible operation, the accuracy of two groups steps lower than whose reversible operation applies. It indicates the incomplete compensation of subsequent training for watermarked model using, but is complete by reversible operation. iii) We observe that group A is affected severely than group B after watermark embedding, and reaches a slower plateau in subsequent training, implying higher effectiveness for reversible operation in group A.

To analyze the specific effects of the proposed method's various processes, we compare the values of original, watermarked and recovered weights for two

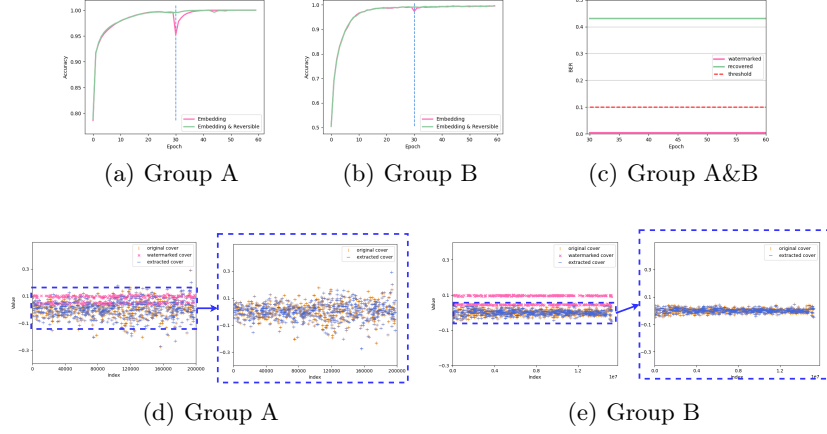


Fig. 8: Simulations on recovering performance. (a) (b) Effects on recovering operation while training for 60 epochs and embedding at epoch 30. (c) Detecting results of watermark before and after recovering. (d) (e) Values comparison on original, watermarked and recovered weights.

combinations in Fig. 8(c). In Fig.8(c), the point of original and recovered cover (represented by horizontal line and vertical bar) are coincided at each index of sample, indicating correct recovery. Meanwhile, the distribution of watermarked weights (represented by cross) in Fig. 8(c) shows the impact on the weights caused by watermark embedding.

Finally, as the legitimacy authentication function is related to determining whether the restored DNN model contains a watermark, we compared the bit error rate (BER) metric of the watermark with and without the reversible operation depicted in Fig. 8(d), (e). The BER value of the watermarked model is 0.0005, whereas it is 0.43 after applying reversible operation. This confirms that the reversible operation can effectively remove the watermark embedded in the host model, thereby demonstrating the validity of the legitimacy authentication scheme.

6 CONCLUSIONS

In this paper, a new static DNN watermarking scheme, referred to as reversible QIM (R-QIM), has been proposed. The watermarked DNN model enjoys higher capacity and fidelity, and no weaknesses on the usability of host data under any distribution. We have also proposed two R-QIM based schemes to realize integrity protection and infringement identification of DNNs. The integrity protection scheme allows the integrity of watermarked DNNs to be verified by determining the difference between restored and original model. In infringement identification, whether current user is legal can be confirmed by detecting the

existence of watermarks contained in the watermarked model. Theoretical analyses and numerical simulations show that R-QIM is more competitive than the method in [4], in terms of its more flexible fidelity performance, high embedding capacity, and adaptability to the weights of arbitrary distribution.

References

1. Barni, M., Pérez-González, F., Tondi, B.: DNN watermarking: Four challenges and a funeral. In: Borghys, D., Bas, P., Verdoliva, L., Pevný, T., Li, B., Newman, J. (eds.) *IH&MMSec '21: ACM Workshop on Information Hiding and Multimedia Security*, Virtual Event, Belgium, June, 22-25, 2021. pp. 189–196. ACM (2021). <https://doi.org/10.1145/3437880.3460399>
2. Chen, B., Wornell, G.W.: Quantization index modulation: A class of provably good methods for digital watermarking and information embedding. *IEEE Trans. Inf. Theory* **47**(4), 1423–1443 (2001). <https://doi.org/10.1109/18.923725>
3. Fei, J., Xia, Z., Tondi, B., Barni, M.: Supervised GAN watermarking for intellectual property protection. In: *IEEE International Workshop on Information Forensics and Security, WIFS 2022, Shanghai, China, December 12-16, 2022*. pp. 1–6. IEEE (2022). <https://doi.org/10.1109/WIFS55849.2022.9975409>
4. Guan, X., Feng, H., Zhang, W., Zhou, H., Zhang, J., Yu, N.: Reversible watermarking in deep convolutional neural networks for integrity authentication. In: *Proceedings of the 28th ACM International Conference on Multimedia*. ACM (oct 2020). <https://doi.org/10.1145/3394171.3413729>
5. Hua, G., Huang, J., Shi, Y.Q., Goh, J., Thing, V.L.L.: Twenty years of digital audio watermarking - a comprehensive review. *Signal Process.* **128**, 222–242 (2016). <https://doi.org/10.1016/j.sigpro.2016.04.005>
6. Krizhevsky, A., Hinton, G., et al.: Learning multiple layers of features from tiny images. Master's thesis, University of Tront (2009)
7. Kuribayashi, M., Tanaka, T., Suzuki, S., Yasui, T., Funabiki, N.: White-box watermarking scheme for fully-connected layers in fine-tuning model. In: *Proceedings of the 2021 ACM Workshop on Information Hiding and Multimedia Security*. pp. 165–170 (2021)
8. LeCun, Y., Cortes, C.: "mnist handwritten digit database", <http://yann.lecun.com/exdb/mnist/>
9. Li, Y., Abady, L., Wang, H., Barni, M.: A feature-map-based large-payload DNN watermarking algorithm. In: Zhao, X., Piva, A., Alfaro, P.C. (eds.) *Digital Forensics and Watermarking - 20th International Workshop, IWDW 2021, Beijing, China, November 20-22, 2021, Revised Selected Papers*. Lecture Notes in Computer Science, vol. 13180, pp. 135–148. Springer (2021). https://doi.org/10.1007/978-3-030-95398-0_10
10. Li, Y., Tondi, B., Barni, M.: Spread-transform dither modulation watermarking of deep neural network. *Journal of Information Security and Applications* **63**, 103004 (2021)
11. Li, Y., Wang, H., Barni, M.: A survey of deep neural network watermarking techniques. *Neurocomputing* **461**, 171–193 (2021)
12. Lou, S., Deng, J., Lyu, S.: Chaotic signal denoising based on simplified convolutional denoising auto-encoder. *Chaos, Solitons & Fractals* **161**, 112333 (2022). <https://doi.org/https://doi.org/10.1016/j.chaos.2022.112333>

13. Lyu, S., Wang, Z., Ling, C., Chen, H.: Better lattice quantizers constructed from complex integers. *IEEE Trans. Commun.* **70**(12), 7932–7940 (2022). <https://doi.org/10.1109/TCOMM.2022.3215685>
14. Moulin, P., Koetter, R.: Data-hiding codes. *Proc. IEEE* **93**(12), 2083–2126 (2005). <https://doi.org/10.1109/JPROC.2005.859599>
15. Ni, Z., Shi, Y., Ansari, N., Su, W.: Reversible data hiding. *IEEE Trans. Circuits Syst. Video Technol.* **16**(3), 354–362 (2006). <https://doi.org/10.1109/TCSVT.2006.869964>
16. Pagnotta, G., Hitaj, D., Hitaj, B., Perez-Cruz, F., Mancini, L.V.: Tattooed: A robust deep neural network watermarking scheme based on spread-spectrum channel coding. *arXiv preprint arXiv:2202.06091* (2022)
17. Qin, J., Lyu, S., Deng, J., Liang, X., Xiang, S., Chen, H.: A lattice-based embedding method for reversible audio watermarking. *arXiv preprint arXiv:2209.07066* (2022). <https://doi.org/10.48550/ARXIV.2209.07066>
18. Shi, Y., Li, X., Zhang, X., Wu, H., Ma, B.: Reversible data hiding: Advances in the past two decades. *IEEE Access* **4**, 3210–3237 (2016). <https://doi.org/10.1109/ACCESS.2016.2573308>
19. Tang, W., Li, B., Barni, M., Li, J., Huang, J.: An automatic cost learning framework for image steganography using deep reinforcement learning. *IEEE Trans. Inf. Forensics Secur.* **16**, 952–967 (2021). <https://doi.org/10.1109/TIFS.2020.3025438>
20. Thodi, D.M., Rodríguez, J.J.: Prediction-error based reversible watermarking. In: *Proceedings of the 2004 International Conference on Image Processing, ICIP 2004, Singapore, October 24–27, 2004*. pp. 1549–1552. IEEE (2004)
21. Tian, J.: Reversible data embedding using a difference expansion. *IEEE Trans. Circuits Syst. Video Technol.* **13**(8), 890–896 (2003). <https://doi.org/10.1109/TCSVT.2003.815962>
22. Uchida, Y., Nagai, Y., Sakazawa, S., Satoh, S.: Embedding watermarks into deep neural networks. In: *Proceedings of the 2017 ACM on international conference on multimedia retrieval*. pp. 269–277 (2017)
23. Wu, X., Sun, W.: High-capacity reversible data hiding in encrypted images by prediction error. *Signal Process.* **104**, 387–400 (2014). <https://doi.org/10.1016/j.sigpro.2014.04.032>
24. Zamir, R.: *Lattice Coding for Signals and Networks: A Structured Coding Approach to Quantization, Modulation, and Multiuser Information Theory*. Cambridge University Press (2014)